

Higgs results in the $WW^{(*)} \rightarrow l\nu l\nu$ decay channel at ATLAS

M. TESTA on behalf of the ATLAS COLLABORATION

INFN, Laboratori Nazionali di Frascati - Frascati (RM), Italy

ricevuto l'1 Ottobre 2013

Summary. — In this paper the evidence of a Higgs-like boson candidate in the $H \rightarrow WW \rightarrow l\nu l\nu$ channel, observed by the ATLAS experiment at the LHC, is presented. The data sample used corresponds to an integrated luminosity of 20.7 fb^{-1} at a center-of-mass energy of 8 TeV and 4.6 fb^{-1} at 7 TeV. The analyses focuses on the search of the Standard Model Higgs Boson with $m_H = 125 \text{ GeV}$. The significance of the observed excess of events over the expected number of background events is 3.8; the expected value is 3.7. The ratio between the observed and expected numbers of events is consistent with unity, $\mu = 1.0 \pm 0.31$.

PACS 14.80.Bn – Standard-model Higgs bosons.

1. – Introduction

In the summer of 2012, the ATLAS and CMS experiment discovered a Higgs-like boson with a mass of approximately $m_H = 126 \text{ GeV}$ [1, 2]. Recently the evidence of the Standard Model (SM) Higgs-like boson in the $H \rightarrow WW^{(*)} \rightarrow l\nu l\nu$ channel has been presented by the ATLAS collaboration using the complete data sample of 2012 and 2011 taken at $\sqrt{s} = 8$ and 7 TeV respectively. This channel provides fundamental inputs for the overall production rate and the couplings to weak boson.

2. – Data sample

The data sample used for this analysis was collected using the ATLAS detector [3]. It corresponds to an integrated luminosity of 20.7 fb^{-1} at a center-of-mass energy of 8 TeV and 4.6 fb^{-1} at 7 TeV. Data were triggered requiring at least a muon or an electron with $p_T > 24 \text{ GeV}$. In this analysis, the signal contributions, used in the Monte Carlo (MC) simulation, include the dominant gluon-gluon fusion production process ($gg \rightarrow H$, denoted as ggF), the vector-boson fusion process ($qq' \rightarrow qq'H$, denoted as VBF) and the Higgs-strahlung process ($qq' \rightarrow WH, ZH$, denoted as VH). More information on the MC samples used for the signal and the background processes can be found in [4].

3. – Objects definition and event selection

The experimental signature of $H \rightarrow WW^{(*)} \rightarrow l\nu l\nu$ events is characterized by two high p_T leptons with same flavour (SF), ee and $\mu\mu$, or opposite flavour (OF), $e\mu$ and μe , large missing transverse energy ($\mathbf{E}_T^{\text{miss}}$), due to the presence of neutrinos in the final states, and 0,1 or ≥ 2 jets (N_{jets}).

Electron candidate are selected by applying tight identification criteria using a combination of tracking and calorimeter information and are required to be in the range of $|\eta| < 2.47$ excluding $1.37 < |\eta| < 1.52$. Muon candidates are identified by matching track reconstructed in the inner detector and in the muon spectrometer and are required to be in the range $|\eta| < 2.5$. At least on the leptons candidate must match a trigger object. Jets are reconstructed using the anti- k_t algorithm with distance parameter $R = 0.4$ and are required to have $p_T > 25$ GeV if $|\eta| < 2.4$ and $p_T > 30$ GeV if $2.4 < |\eta| < 4.5$. $\mathbf{E}_T^{\text{miss}}$ is computed from the negative vectorial sum of the muon, electrons, photons, jets, and clusters of calorimeter cells not associated to these objects. For events in the $N_{jet} \leq 1$ modes, a requirement is made on $E_{T,rel}^{\text{miss}}$, which is defined as: $E_{T,rel}^{\text{miss}} = E_T^{\text{miss}} \times \sin(\Delta\phi_{min})$ where $\phi_{min} = \min(\Delta\phi, \pi/2)$ and $\Delta\phi$ is the azimuthal angular difference between the $\mathbf{E}_T^{\text{miss}}$ vector and the nearest candidate leptons or jet. Due to large amount of Drell-Yan (DY) background with fake $\mathbf{E}_T^{\text{miss}}$ in events with many pile-up interactions, additional variables are used to further reduce this background: $\mathbf{p}_T^{\text{miss}}$, a track-based measurement of the missing transverse momentum, reconstructed selecting tracks from the primary interaction and f_{recoil} , the soft hadronic recoil opposite to the di-lepton system and any accompanying jet for $N_{jet} \leq 1$. Detailed information on the objects definition and on the events selection can be found in [4].

Since the rate and background composition depend on the jet multiplicity, the analysis has been splitted in bins of in N_{jet} .

For $N_{jet} \leq 1$ the signal originates from the ggF process and WW events dominate the background composition. For $N_{jet} \geq 2$ the signal comes mostly from the VBF process and $t\bar{t}$ events dominate the background. For all jet multiplicities, topological cuts are applied. Due to spin correlation in the $H \rightarrow WW^{(*)}$ decay and the $V - A$ structure of the W decay, the two leptons emerge in the same direction. The leptons invariant mass is therefore required to be small, $m_{ll} < 50$ GeV for $N_{jet} \leq 1$ and $m_{ll} < 60$ GeV for $N_{jet} \geq 2$ and their azimuthal separation is required to be small, $|\Delta\phi_{ll}| < 1.8$. In the $N_{jet} = 0$ analysis for the OF channel, a cut on $E_{T,rel}^{\text{miss}} > 25$ GeV is applied. For the SF channel the selection is tighter, because of the large Z/γ^* background: $E_{T,rel}^{\text{miss}} > 25$ GeV and $p_{T,rel}^{\text{miss}} > 45$ GeV and the hadronic recoil is required to be small, $f_{recoil} < 0.05$. The transverse momentum of the di-leptons system is required to be large, $p_T^{ll} > 30$ GeV. In the $N_{jet} = 1$ analysis, the $E_{T,rel}^{\text{miss}}$ and $p_{T,rel}^{\text{miss}}$ requirements are the same as in $N_{jet} = 0$, but the requirement on hadronic recoil is looser, $f_{recoil} < 0.2$. The top background is suppressed by rejecting events with a heavy-flavour jet identified with a multi-variate b -tagging algorithm. The $Z/\gamma^* \rightarrow \tau\tau$ background in OF channel is reduced using the invariant mass calculated for the τ hypothesis, $|m_{\tau\tau} - m_Z| > 25$ GeV. In the $N_{jet} \geq 2$ analysis, the VBF-specific kinematics of the two highest- p_T jets in the event (tag jets) are used. Their rapidity gap is required to be large, $\Delta y_{jj} > 2.8$ and their invariant mass is required to be high, $m_{jj} > 500$ GeV. To reduce ggF contributions, events with a jet with $p_T > 20$ GeV inside the rapidity gap are vetoed. $t\bar{t}$ background is suppressed by requiring a small total transverse moment, $p_T^{\text{tot}} < 45$ GeV, where $\mathbf{p}_T^{\text{tot}} = \mathbf{p}_T^{ll} + \mathbf{p}_T^{jj} + \mathbf{E}_T^{\text{miss}}$, where $\mathbf{p}_T^{\text{tot}}$ is the vectorial sum of the transverse momenta of the tag jets.

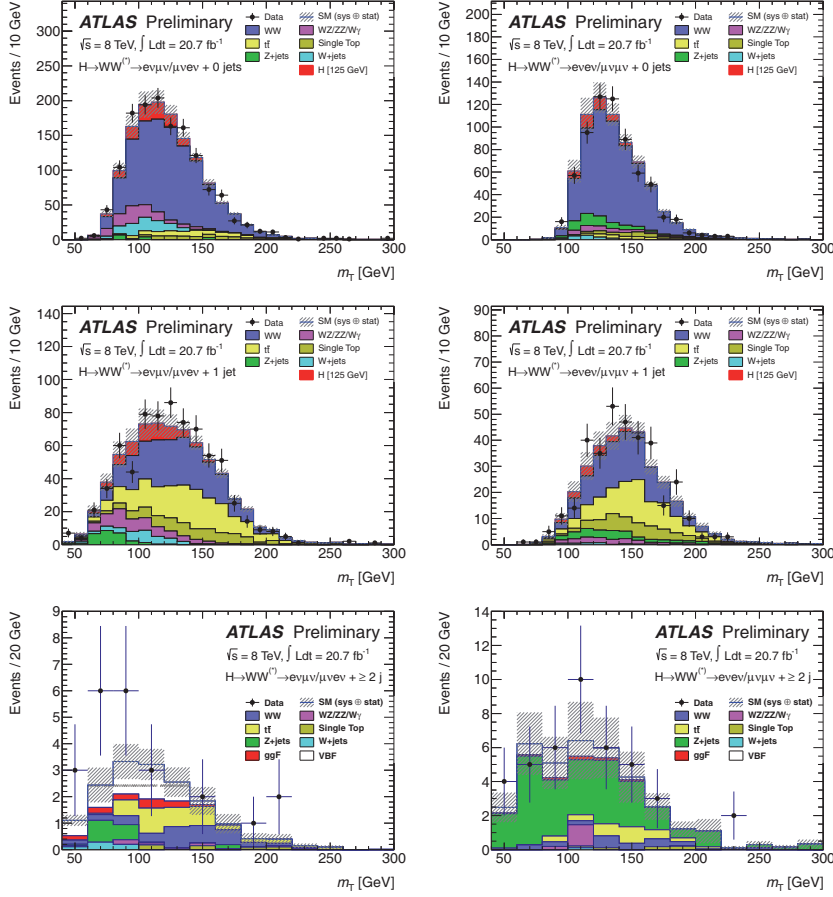


Fig. 1. – Distributions for the transverse mass, m_T , for 8 TeV data. The plots are shown for the $e\mu + \mu e$ (left) and $ee + \mu\mu$ (right) channels in the $N_{jet} = 0$ (top), $N_{jet} = 1$ (middle), $N_{jet} \geq 2$ (bottom) modes. For the $N_{jet} \geq 2$ mode, the signal is plotted separately for ggF and VBF production processes.

4. – Background estimation

Background yields are estimated in control region using correction from the MC simulation. The Z/γ^* yield is estimated from data using a combination of $\mathbf{E}_T^{\text{miss}}$, $\mathbf{p}_T^{\text{miss}}$ and f_{recoil} with uncertainties of 60%, 80% and 15% in the $N_{jet} = 0, 1, \geq 2$ analyses, respectively. The top background ($t\bar{t}$ + single top process) is evaluated in a data control region, defined by reversing the b -jet veto and removing the requirements on $\Delta\Phi_{ll}$ and m_{ll} . The corresponding uncertainties are 28%, 80% and 39% in the $N_{jet} = 1, \geq 2$ analyses, respectively. The WW continuum background has the same final state of the signal, but different lepton spin correlation. Its yield is evaluated in a control region defined by removing the $\Delta\Phi_{ll}$ cut and requiring $50 < m_{ll} < 100$ GeV for $N_{jet} = 0$ and $m_{ll} > 80$ for $N_{jet} = 1$. In the $N_{jet} = 2$ analysis, the WW background is evaluated using only MC simulation. The corresponding uncertainty are 7.4%, 37% and 37% in the $N_{jet} = 0, 1, \geq 2$ analyses, respectively.

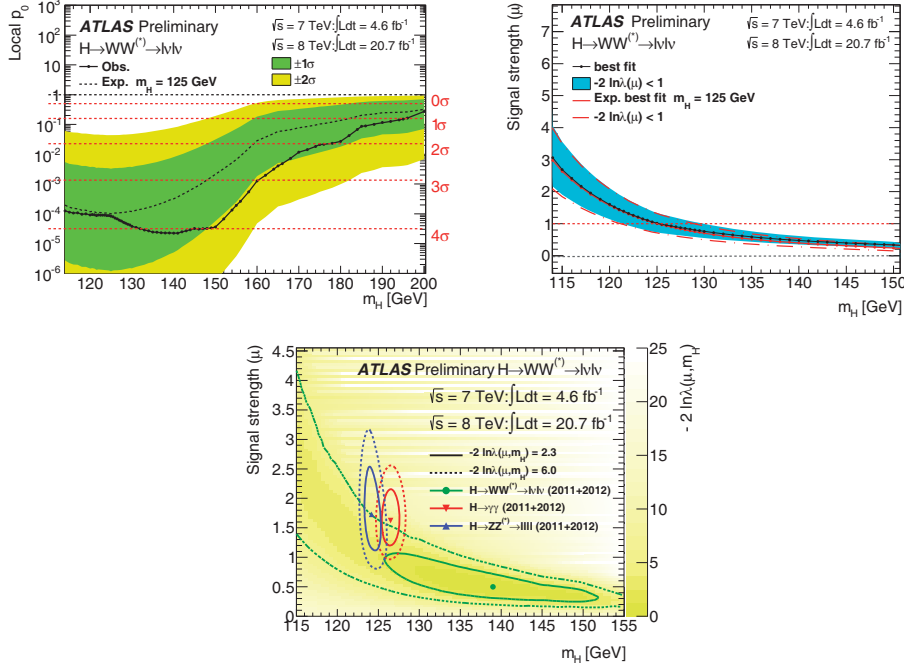


Fig. 2. – Top Left: Results for probability for the background-only scenarios as a function of m_H . Smaller green bands represent the $\pm 1\sigma$ uncertainties on the expected value, and the larger yellow band represent $\pm 2\sigma$ uncertainties. Top Right: μ value for fitted results (solid black line with shaded cyan band) and for expected result (solid red line with dashed band). Bottom: $\mu - m_H$ likelihood contour: 68% and 95% contour are drawn.

5. – Signal extraction and results

After all cuts described in sect. 3, the $e\mu + \mu e$ sample is further splitted in two signal regions at $0 < m_{ll} < 30$ and $30 < m_{ll} < 50$, because of the different background amount and composition. A fit to the transverse mass, m_T , distribution is then used to extract the signal yield. m_T is defined as $m_T = ((E_T^l + E_T^{\text{miss}})^2 - |\mathbf{p}_T^l + \mathbf{E}_T^{\text{miss}}|^2)^{1/2}$ with $E_T^l = (|\mathbf{p}_T^l|^2 + m_l^2)^{1/2}$. Figures 1 show the expected signal and the backgrounds for the different N_{jet} analyses and decay channels. The expected and observed results are given combining the jet multiplicity. The expected significance of the signal with $m_H = 125$ GeV is 3.7 s.d. ($p_0 = 1 \times 10^{-4}$). The corresponding observed significance is 3.8 s.d. ($p_0 = 8 \times 10^{-5}$) (fig. 2a). The excess of events is quantified for a signal at $m_H = 125$ GeV by the ratio between the observed and expected numbers of signal events $\mu_{obs} = 1.01 \pm 0.21(\text{stat.}) \pm 0.19(\text{theo. syst.}) \pm 0.12(\text{expt. syst.}) \pm 0.04(\text{lumi}) = 1.01 \pm 0.31$. The dominant systematic uncertainties on μ_{obs} are the theoretical uncertainties on the WW background normalization and on the normalization of the signal yield. The experimental uncertainties on μ_{obs} are dominated by the b -tagging efficiency and the jet energy scale and resolution. Figure 2b shows that the observed μ vs. m_H is consistent with the expected distribution in the presence of a signal. Figure 2c shows a scan of the likelihood in the $\mu - m_H$ plane where the $H \rightarrow WW^{(*)} \rightarrow l\nu l\nu$ result is compared to that of $H \rightarrow ZZ^{(*)} \rightarrow 4l$ and $H \rightarrow \gamma\gamma$.

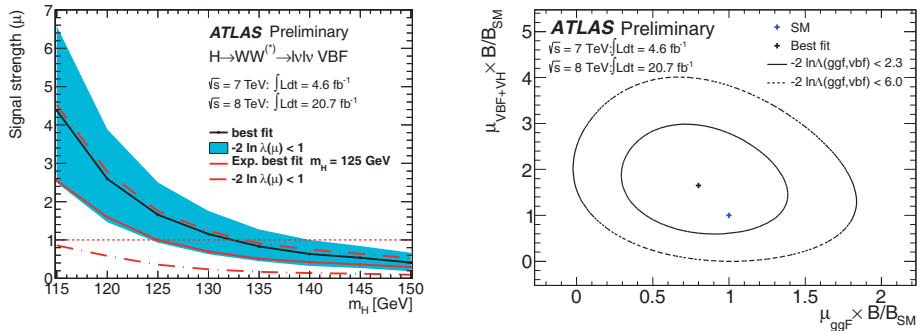


Fig. 3. – Left: VBF signal strength parameter μ . The observed (solid black line with shaded cyan band) and the expected result (solid red line with dashed band) are shown. Right: Likelihood contours and best-fit value for μ_{ggF} and μ_{VBF} . 68% and 95% contour are shown.

The measured value of the product of the cross section and the $WW^{(*)}$ branching ratio for a signal at $m_H = 125$ GeV at 8 TeV is 6.0 ± 1.6 pb, while the expected value is 4.8 ± 0.7 pb. The results are consistent with the prediction for the Standard Model Higgs boson decaying to a pair of W .

Statistical test of a VBF signal are performed by considering the ggF signal as part of the background, and the signal strength associated with the VBF process, μ_{VBF} , as the parameter of interest. The expected VBF signal significance at $m_H = 125$ GeV is 1.6 s.d. ($p_0 = 0.05$), and the corresponding observed significance is 2.5 s.d. ($p_0 = 0.07$). A 2D simultaneous fit is performed to measure $\mu_{obs,VBF}$ and $\mu_{obs,ggF}$. The best-fit measured single strength for VBF process at $m_H = 125$ GeV is: $\mu_{obs,VBF} = 1.66 \pm 0.67(stat.) \pm 0.42(syst.) = 1.66 \pm 0.79$ and for ggF process: $\mu_{obs,ggF} = 0.82 \pm 0.24(stat.) \pm 0.28(syst.) = 0.82 \pm 0.36$. Figure 3a shows μ_{VBF} vs. m_H . A two-dimensional likelihood scan of the signal strength for the ggF and VBF production modes are shown in fig. 3b. The results are consistent with the expected SM values of unity.

REFERENCES

- [1] ATLAS COLLABORATION, *Phys. Lett. B*, **716** (2012) 1.
- [2] CMS COLLABORATION, *Phys. Lett. B*, **716** (2012) 30.
- [3] ATLAS COLLABORATION, *JINST*, **3** (2008) S08003.
- [4] ATLAS COLLABORATION, “Measurements of the properties of the Higgs-like boson in the $W \rightarrow \nu\nu\nu$ decay channel with the ATLAS detector using 25 fb^{-1} of proton-proton collision data”, ATLAS-CONF-2013-030.